Anal Bioanal Chem (2012) 402:2407–2415
DOI 10.1007/s00216-011-5705-9

ORIGINAL PAPER

Particle size measurement of lipoprotein fractions using diffusion-ordered NMR spectroscopy

Roger Mallol · Miguel A. Rodríguez · Mercedes Heras · Maria Vinaixa · Núria Plana · Lluís Masana · Gareth A. Morris · Xavier Correig

Received: 26 October 2011 / Revised: 21 December 2011 / Accepted: 29 December 2011 / Published online: 1 February 2012

Abstract The sizes of certain types of lipoprotein particles have been associated with an increased risk of cardiovascular disease. However, there is currently no gold standard technique for the determination of this parameter. Here, we propose an analytical procedure to measure lipoprotein particles sizes using diffusion-ordered nuclear magnetic resonance spectroscopy (DOSY). The method was tested on six lipoprotein fractions, VLDL, IDL, LDL_1, LDL_2, HDL_2, and HDL_3, which were obtained by sequential ultracentrifugation from four patients. We performed a pulsed-field gradient experiment on each fraction to obtain a mean diffusion coefficient, and then determined the apparent hydrodynamic radius using the Stokes–Einstein equation. To validate the hydrodynamic radii obtained, the particle size distribution of these lipoprotein fractions was also measured using transmission electron microscopy (TEM). The standard errors of duplicate measurements of diffusion coefficient ranged from 0.5% to 1.3%, confirming the repeatability of the technique. The coefficient of determination between the hydrodynamic radii and the TEM-derived mean particle size was $r^2=0.96$, and the agreement between the two techniques was 85%. Thus, DOSY experiments have proved to be accurate and reliable for estimating lipoprotein particle sizes.

Keywords Lipoprotein · NMR · DOSY · TEM

Abbreviations

CVD	Cardiovascular disease
DOSY	Diffusion-ordered NMR spectroscopy
DSTE	Double-stimulated echo
GGE	Gradient gel electrophoresis
HDL	High-density lipoprotein
IDL	Intermediate density lipoprotein
LDL	Low-density lipoprotein
LED	Longitudinal eddy current delay
LS	Light scattering
NMR	Nuclear magnetic resonance
PFG	Pulsed-field gradient
RMSPE	Root mean squared percentage error
sdLDL	Small, dense LDL
SE	Standard error
SNR	Signal-to-noise ratio
TEM	Transmission electron microscopy
TSP	3-Trimethylsilyl[2,2,3,3-d_4]propionate
VLDL	Very low-density lipoprotein

Electronic supplementary material The online version of this article (doi:10.1007/s00216-011-5705-9) contains supplementary material, which is available to authorized users.

R. Mallol (✉) · M. Vinaixa · X. Correig
Department of Electronic Engineering, Universitat Rovira i Virgili,
Avinguda Països Catalans 26,
43007 Tarragona, Spain
e-mail: roger.mallol@urv.cat

R. Mallol · M. A. Rodríguez · M. Vinaixa · X. Correig
Metabolomics Platform, IISPV, Universitat Rovira i Virgili,
Avinguda Països Catalans 26,
43007 Tarragona, Spain

R. Mallol · M. A. Rodríguez · M. Heras · M. Vinaixa · N. Plana · L. Masana · X. Correig
CIBERDEM,
Carrer Mallorca 183,
08036 Barcelona, Spain

M. Heras · N. Plana · L. Masana
Lipids and Atherosclerosis Research Unit,
Sant Joan University Hospital, IISPV, Universitat Rovira i Virgili,
Carrer Sant Llorenç 21,
43201 Reus, Spain

G. A. Morris
School of Chemistry, University of Manchester,
Manchester M13 9PL, UK

Introduction

Interest in the assessment of the size profiles of lipoprotein particles has been increasing due to the role of this parameter in cardiovascular disease (CVD) risk prediction [1]. For example, small, dense low-density lipoprotein (sdLDL) particles are removed slowly from the blood stream, which subjects them to oxidation processes and leads to the formation of atheroma [2, 3]. Moreover, a predominance of sdLDL is associated with an atherogenic lipoprotein phenotype that is characterized by high concentrations of plasma triglyceride, low concentrations of high-density lipoprotein (HDL) cholesterol and apoA-I, and high insulin resistance [4–7]. In contrast, HDL particles are considered to be antiatherogenic lipoproteins because they help reverse cholesterol transport [8, 9]. In addition, when HDL particles are divided into large and small HDL subclasses, a decrease in the number of larger particles has a stronger influence on the development of CVD. The summary described above is based on several epidemiological studies; however, other studies contribute to the controversy regarding (1) whether sdLDL particle numbers may be considered an independent risk factor for CVD, (2) which HDL subclasses are more protective against CVD, and (3) whether new lipoprotein analytical methods improve risk assessment compared with standard lipid panels [10–13].

Several methods have been developed to determine the particle sizes of different lipoprotein fractions. The Vertical Auto Profile-II or VAP-II test (Atherotec Inc.) fractionates lipoproteins on the basis of differences in density [14]. In contrast, the nuclear magnetic resonance (NMR) LipoProfile-II test (LipoScience Inc.) distinguishes among the different lipoprotein particles using the chemical shift value of the methyl NMR signal [15]. Lipoprotein particle sizes are then estimated based on a proprietary library containing the NMR signals of lipoproteins of known size. Other methods are based on gradient gel electrophoresis (GGE), including segmented GGE (Berkeley HeartLab), which separates lipoproteins based on their size, and the Quantimetrix Lipoprint LDL System, which estimates LDL particle sizes by comparing their electrophoretic mobility to the electrophoretic mobilities of particles of known size [16, 17]. All of the methods described above are based on different physicochemical properties, which make them difficult to compare. In addition, they estimate lipoprotein sizes using different assumptions and approximations. Consequently, recent reviews have emphasized their divergence [18–22]. A recent study by Ensign et al. that compared the LDL particle sizes obtained using these four methods reported a total agreement of only up to 8% according to LDL subclass phenotyping (preponderance of large, intermediate, or small LDL particles) [19]. Clearly, there is a need for standardization [23]. Another disadvantage of the methods that are currently available is that information is delivered on a reduced set of lipoprotein subclasses. Because LDL is usually considered the most clinically relevant lipoprotein class, most of the studies published to date have been focused on LDL phenotyping, and other lipoprotein classes, such as very low-density lipoprotein (VLDL) or intermediate density lipoprotein (IDL), are seldom reported. Therefore, it would be beneficial to consider a complete profile of lipoprotein particle sizes.

In order to measure lipoprotein particles sizes, diffusion-ordered NMR spectroscopy (DOSY) might be thought as a good alternative due to its robustness and simple sample manipulation [24–26]. DOSY has been extensively used to measure the size distribution of different materials, including lipid vesicles and gold nanoparticles [27, 28]. In this study, the particle sizes of six lipoprotein fractions, VLDL, IDL, LDL_1, LDL_2, HDL_2, and HDL_3, were assessed using DOSY. To the best of our knowledge, this is the first reported work that attempts to assess the particle sizes of ultracentrifuged lipoprotein fractions using this technique. First, the attenuation of the methyl signal was used to obtain a diffusion coefficient for each fraction. We evaluated the diffusion coefficients that were obtained in terms of the signal-to-noise ratio (SNR), and we then constructed a DOSY schematic map to deliver a qualitative visualization plot for lipoprotein analysis. Second, the hydrodynamic radii of the lipoprotein fractions (R_H) were derived using the Stokes–Einstein equation [24]:

$$R_H = \frac{kT}{6\pi\eta D} \tag{1}$$

where k is the Boltzmann constant, T is the absolute temperature, and η is the solvent or solution viscosity. Equation 1 can be decomposed into its component pieces, i.e., the Einstein relationship between a thermal, stochastic property (diffusivity) and a deterministic, mechanical property (mobility) [29]:

$$M = \frac{D}{kT} \tag{2}$$

and the Stokes relationship that relates the deterministic probe response (mobility) to the rheological properties of the material (viscosity):

$$R_H = (6\pi\eta M)^{-1} \tag{3}$$

While the Einstein relationship is strictly valid in this study, the Stokes relationship may fail since it assumes infinite dilution conditions and a continuum solvent. To enable some corrections to be made for obstruction effects, we therefore also measured the experimental viscosity. The feasibility of using Eq. 1 will be explored, comparing the

mobility and hydrodynamic radii to the mean lipoprotein sizes measured using transmission electron microscopy (TEM), which has been extensively used in the characterization of lipoprotein fractions [30].

Materials and methods

Patient selection

Four patients attending the Lipid Clinic of Sant Joan University Hospital in Reus with different hyperlipoproteinemic phenotypes to cover a broad range of lipid and lipoprotein concentrations were recruited. Patients 1 and 3 were diabetic and suffered from lipoprotein lipase deficiency (Type I) and severe hypertriglyceridemia (Type V), respectively. Patients 2 and 4 had dis-β-lipoproteinemia (Type III) and polygenic hypercholesterolemia (Type IIa), respectively. Blood samples were obtained after a 12-h overnight fasting period; samples were withdrawn into EDTA-containing tubes and centrifuged immediately for 15 min at 4 °C and 1,500×*g* to obtain plasma. The study protocol was approved by the Ethical Committee of Sant Joan University Hospital. All patients gave their written consent to participate in the research program.

Lipoprotein fractionation

Six lipoprotein fractions were obtained from the collected plasma by sequential preparative ultracentrifugation in a Kontron ultracentrifuge T-1075 rotor TFT 45.6 at 4 °C, as previously described [31]. The lipoproteins isolated included VLDL (0.95–1.006 g/ml), IDL (1.006–1.019 g/ml), LDL_1 (1.019–1.044 g/ml), LDL_2 (1.044–1.063 g/ml), HDL_2 (1.063–1.0125 g/ml), and HDL_3 (1.125–1.210 g/ml). Sucrose was added to the samples to maintain the physicochemical properties of all the fractions prior to freezing, as previously described [32]. All lipoprotein fractions were concentrated two-fold prior to NMR analysis, with the exception of the LDL_2 fraction of patient 2.

The total cholesterol and levels of triglycerides, direct LDL cholesterol, HDL cholesterol, and ApoB-100 in the plasma samples, as well as the lipid and apolipoprotein levels in the lipoprotein fractions, were measured using enzymatic and immunoturbidimetric assays. In Electronic Supplementary Material Table S1, the analytical lipid and lipoprotein values are detailed.

Diffusion-ordered NMR spectroscopy (DOSY)

To prepare samples for DOSY, the lipoprotein fractions (430 μl) were transferred into NMR tubes (o.d. 5 mm). An internal reference tube (o.d. 2 mm, supported by a Teflon adapter) containing 9.9 mmol/l sodium 3-trimethylsilyl [2,2,3,3-d_4]propionate (TSP) and 0.47 mmol/l $MnSO_4$ in 99.9% D_2O was placed coaxially into the NMR sample tube. The tubes were maintained at 4 °C in the sample changer until the time of analysis.

^{1}H NMR spectra were recorded on a Bruker Avance III 600 spectrometer operating at 600.20 MHz. Diffusion measurements were performed at 310 K to obtain a full signal from the melted lipids in the lipoproteins and to avoid serum degradation during measurement. The double-stimulated echo (DSTE) pulse program was used, with bipolar gradient pulses and a longitudinal eddy current delay (LED) [33]. This pulse program consists of a DSTE sequence followed by z-storage of the magnetization, and allows longer diffusion delays that are limited only by the longitudinal relaxation of the molecules. This requirement is compulsory if the pulse sequence is to be applied to lipoproteins, in which $T_1 >> T_2$. A DSTE sequence efficiently compensates for flow convection currents that can develop in plasma samples at elevated temperatures. Additionally, three spoil gradient pulses were employed during the z-storage periods and during the recycle delay, to shorten the phase cycle and eliminate accidental refocusing of unwanted magnetization. To minimize the possibility of convection currents, the heating air flow rate was set to 670 l/h. A spectral window of 18,000 Hz was used, with an acquisition time of 1.82 s.

During the experiment, the relaxation delay was 2 s, the FIDs were collected into 64 k complex data points, and 32 scans were acquired for each sample. The gradient pulse strength was increased from 5% to 95% of the maximum strength of 53.5 Gcm^{-1} in 50 steps, in which the squared gradient pulse strength was exponentially distributed. A diffusion time (Δ) of 120 ms and bipolar half-sine-shaped gradient pulses (δ) of 6 ms were applied to obtain a reasonable amount of lipoprotein signal attenuation:

$$I = I_0 e^{-kDG^2} \tag{4}$$

where $k = (2a\gamma\delta)^2(\Delta - 5\delta/4 - \tau)$, $a=(2/\pi)$ is a gradient shape factor for the half-sine shape, and τ is the short delay between the pulses in a gradient pulse pair. The total experiment time was 1 h 45 min per sample. All spectra were Fourier transformed after applying an exponential function equivalent to 2 Hz Lorentzian line broadening, phase corrected, baseline corrected, and referenced to the TSP reference signal at 0 ppm. The SNR was defined as the ratio of the methyl signal maximum in the least attenuated (lowest gradient) spectrum to the standard deviation of the noise height in the baseline.

Diffusion coefficients were obtained using a surface fitting approach, as described previously [34]. In this case, only one Lorentzian function was used to fit the methyl surface (Fig. 1). The estimated diffusion coefficients and

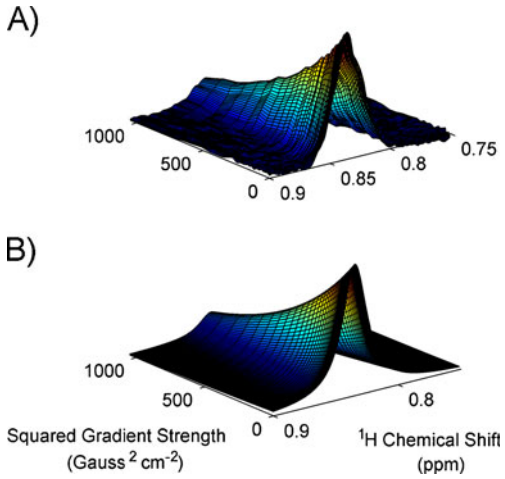

Fig. 1 Surface fitting of the attenuated methyl signal of a VLDL fraction (**A**) using an individual Lorentzian function (**B**)

peak positions were used, together with their standard errors (SE), to build a schematic DOSY peak map showing the distribution of the different lipoprotein fractions in terms of their chemical shifts and diffusion coefficients.

Viscosity measurements

Lipoprotein solution viscosities were measured at 37 °C with a Cannon–Manning semi-micro capillary viscometer. To obtain the viscosity in millipascal seconds, the density of each fraction was calculated by weighing a volume of 250 μL. The kinematic viscosity was then measured by multiplying the efflux time of the sample between two reference lines by the viscometer constant provided by the manufacturer. Finally, the kinematic viscosity and the density were multiplied to obtain the viscosity.

Transmission electron microscopy (TEM)

TEM samples were prepared by placing a drop of each lipoprotein fraction onto a formvar carbon film for 2 min and then blotting the excess liquid. Negative staining was performed with 2% phosphotungstic acid adjusted to pH 6.6; this solution was applied for 1 min and then blotted dry. The gridded samples were examined on a JEOL JEM-1011 TEM at an accelerating voltage of 80 kV. The particle sizes of the lipoprotein fractions were calculated using the IMAQ Vision software (National Instruments Inc.). Each lipoprotein fraction was analyzed using a different number of micrographs. Some images were filtered with a Gaussian filter prior to analysis to avoid interference from noise. All images were then truncated to black and white, and particles at the borders were discarded. All particles with a circularity factor close to 1 were selected. The number of particles considered ranged from 100 to 800. The HDL fractions were particularly difficult to measure via TEM; only the HDL_2 fraction from patient 2 and the HDL_3 fractions of patients 2 and 3 were entered in the regression analysis because these samples were the only HDL fractions that exhibited reasonable particle sizes.

Statistical analysis

The diffusion coefficients among the lipoprotein subclasses were compared using the nonparametric Kruskal–Wallis test. The resulting P value was used to test the null hypothesis of all the subfractions belonging to the same subclass. $P<0.05$ was considered to be statistically significant in order to reject the null hypothesis. A simple linear regression analysis was used to examine the relationship between the lipoprotein mobilities and hydrodynamic radii obtained via NMR, and the lipoprotein particle sizes obtained via TEM. The parameters used to evaluate the linear regressions were the coefficient of determination ($0\leq r^2\leq 1$) and the regression lines. In order to evaluate the agreement between the two techniques, the root mean squared percentage error (RMSPE) of the differences between NMR and TEM was calculated according to the following formula:

$$\mathrm{RMSPE}\ (\%) = \sqrt{\frac{\sum_{1}^{n}\left(\frac{(\mathrm{NMR}-\mathrm{TEM})\times 100}{\mathrm{TEM}}\right)^2}{n}} \qquad (5)$$

where NMR refers to the NMR-derived sizes, TEM to the TEM-derived sizes, and n the number of lipoprotein fractions. All of the analyses were performed with MATLAB Version 7.10.0.499 R2010a (MathWorks).

Results

Calculation of the diffusion coefficients

DOSY experiments are vulnerable to some experimental limitations, such as non-uniform field gradients, temperature gradients, and low solute concentrations [25]. The last limitation is of particular concern in the analysis of lipoprotein fractions because these are typically diluted during several sample manipulation steps; consequently, pulsed-field gradient (PFG) experiments on lipoprotein fractions may yield spectra with low SNR. The VLDL and HDL_3 fractions of patient 1 were therefore evaluated, as they represent two extreme cases for SNR (250:1 and 15:1, respectively). Figure 2A, B illustrates the attenuation of the methyl signal of these samples in a PFG experiment. While the VLDL fraction did not exhibit complete attenuation of the signal over the range of gradient amplitudes used, the HDL_3 fraction was completely attenuated at high gradient strengths

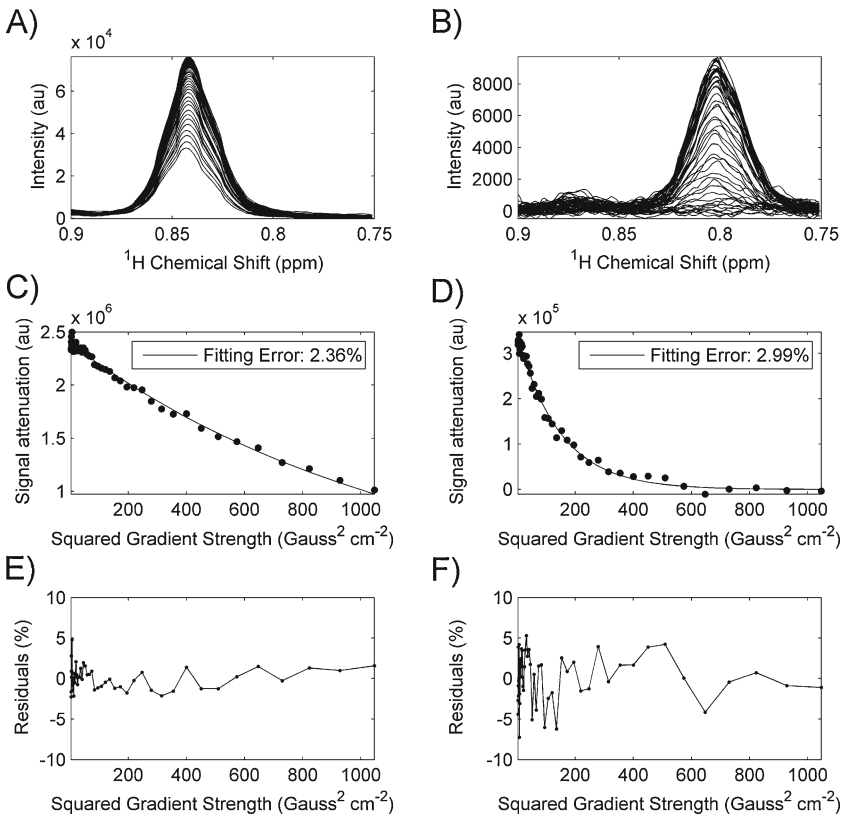

Fig. 2 SNR analysis of DOSY spectra. **A**, **B** Signal attenuation of the VLDL and HDL_3 fractions from patient 1. **C**, **D** Fitting of the integral area to Eq. 4. **E**, **F** Residuals of the fittings

because of the faster diffusion of their particles. The HDL_3 fraction also exhibited lower SNR even at low gradient strengths. The SNR differences between the VLDL and HDL_3 fractions arose because of the different concentrations; the VLDL fraction of patient 1 contained 1.31 and 3.66 mmol/L of cholesterol and triglycerides, respectively, whereas the HDL_3 fraction from the same patient contained 0.16 and 0.09 mmol/L, respectively (see Electronic Supplementary Material Table S1). Despite the low concentrations found in the HDL_3 fraction, the nonlinear least squares fitting of the experimental data to Eq. 4 yielded an acceptable fitting error of ~3% (Fig. 2C–F). The use of integral area attenuation to fit with Eq. 4, instead of intensity attenuation as is more common in DOSY experiments, reduces the amount of uncertainty in signal attenuation due to noise.

Figure 3 shows a schematic DOSY peak map of the diffusion coefficients that were obtained for all the fractions, details of which are also summarized in Table 1. Spectra of the different lipoprotein fractions from patient 3 are shown along the top as a reference. On the right side, projections of the diffusion coefficients are depicted. For each patient, the methyl signal of the neutral lipids in the lipoprotein shows faster diffusion as the lipoprotein densities increase. In general, larger lipoprotein subclasses yielded lower SEs. The maximum SE value of an estimated diffusion coefficient was ~4%, and was obtained for the LDL_2 fraction of patient 2; the estimated SE for the remaining samples was less than 1.5%. A high SE was observed for this particular LDL_2 fraction because it was highly diluted compared with the

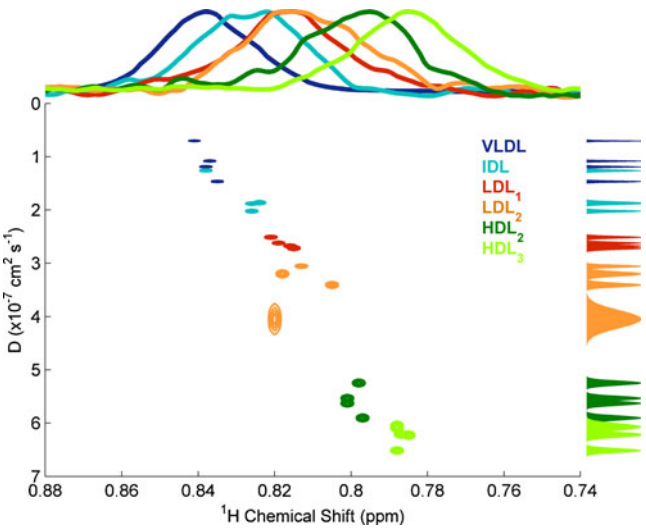

Fig. 3 Schematic DOSY peak map showing the diffusion coefficients obtained by fitting Eq. 4 to each dataset. The width along the chemical shift axis of the Gaussian curves represents the SE in estimating the position, while the width along the diffusion dimension represents the SE in estimating the diffusion coefficient. The superimposed spectra at the top of the figure are those acquired for the lipoprotein fractions from patient 3 and have been normalized for visualization purposes; the Gaussian functions at the right side correspond to the projection of the diffusion spectra obtained for all samples

Table 1 Results from all of the measurements

Fraction	Patient	SNR	D/(cm^2 s^{-1})	M/(cm^2 s^{-1}J^{-1})	η/(mPa s)	R_H/(Å)	TEM size/(Å)
VLDL	1	252	0.70 (0.8)	151	0.81	402	265±113 (400)
	2	208	1.07 (0.8)	233	0.81	261	228±110 (803)
	3	506	1.18 (0.7)	256	1.12	171	136±49 (746)
	4	43	1.46 (0.7)	315	0.80	195	184±44 (625)
IDL	1	14	1.25 (1.0)	271	0.77	236	179±72 (296)
	2	18	2.01 (0.8)	435	0.71	159	169±36 (450)
	3	31	1.88 (0.8)	405	0.87	139	135±26 (106)
	4	17	1.86 (1.0)	401	0.76	160	155±57 (532)
LDL_1	1	14	2.69 (0.9)	585	0.79	107	96±63 (97)
	2	29	2.50 (0.7)	541	0.71	128	114±28 (277)
	3	23	2.66 (0.7)	576	0.77	111	118±36 (95)
	4	45	2.61 (0.6)	564	0.76	114	130±24 (98)
LDL_2	1	11	3.38 (1.0)	734	0.76	88	83±28 (101)
	2	4	4.16 (3.8)	872	0.73	75	86±21 (98)
	3	18	3.05 (0.7)	658	0.85	88	80±19 (162)
	4	9	3.20 (1.3)	689	0.84	84	87±23 (166)
HDL_2	1	25	5.63 (0.7)	1,212	0.77	52	Nd
	2	23	5.89 (0.7)	1,272	0.72	54	45±13 (18)
	3	19	5.23 (0.8)	1,130	0.73	59	Nd
	4	19	5.53 (0.7)	1,192	0.71	58	Nd
HDL_3	1	15	6.09 (1.0)	1,308	0.72	52	Nd
	2	49	6.21 (0.6)	1,338	0.71	51	41±11 (122)
	3	52	6.22 (0.7)	1,341	0.74	49	39±17 (339)
	4	41	6.51 (0.5)	1,403	0.71	49	Nd

D is the diffusion coefficient (percent SE), M is the mobility, η is the viscosity expressed as mean±standard deviation, R_H is the hydrodynamic radii, and the TEM-derived particle sizes are expressed as mean±standard deviation (number of particles measured)

Nd not determined

other fractions; therefore, its SNR (4:1) was around the detection level (5:1). We did not use the diffusion coefficient obtained for this lipoprotein fraction in further analysis.

Lipoprotein subclasses could be clearly distinguished using their average diffusion coefficients (P=0.00073). The minimum difference in diffusion coefficient between two subclasses was 2.8%; the two subclasses involved were the two HDL subclasses. The SE for the fastest HDL_2 fraction and the slowest HDL_3 fraction were 0.7% and 1%, respectively, and these subclasses could still be statistically distinguished (P=0.021). However, there was a lipoprotein fraction that exhibited an average diffusion coefficient that was out of its subclass range. This was the IDL fraction of patient 1, a sufferer from lipoprotein lipase deficiency, and exhibited an average diffusion coefficient within the range of the VLDL fractions. Despite the normal lipid values exhibited by this IDL fraction (see Electronic Supplementary Material Table S1), its low diffusivity suggests that larger and more lipid-rich particles than expected are present. These larger particles may correspond to VLDL particles because complete separation of these lipoprotein fractions by ultracentrifugation cannot be achieved in subjects with this pathology due to the lactescent state of the plasma sample.

Determination and validation of lipoprotein hydrodynamic radii

We obtained a mobility and hydrodynamic radius for each lipoprotein fraction using Eqs. 2 and 3, respectively (Table 1). To evaluate the validity of the Stokes relationship, we performed two linear regression analyses to assess the relationships between the two variables and the TEM-derived particle sizes. Figure 4A illustrates the regression model constructed using the calculated lipoprotein mobilities as a prediction variable. The two variables correlated satisfactorily (r^2=0.78). Using the measured solution viscosity (as a partial correction for the effects of other solution components and of obstruction) and performing the linear regression analysis for hydrodynamic radius instead of mobility resulted in a stronger linear relationship (r^2=0.90), as shown in Fig. 4B. In this figure, dotted rectangles identify the areas in which the different lipoprotein fractions used in this study should be placed according to the literature (VLDL, 150–400 Å; IDL, 125–175 Å; LDL, 90–140 Å; HDL, 25–60 Å) [35]. These rectangles represent the main lipoprotein classes since the size ranges that define the subsequent subclasses are study dependent. As shown in Fig. 4B,

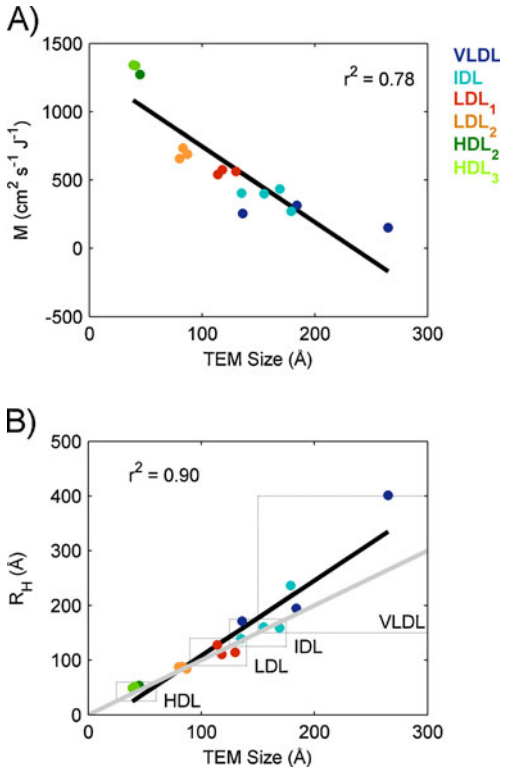

Fig. 4 Regression between NMR-derived data and TEM-derived particle sizes. **A** Relationship between mobility (M) and TEM-derived particle sizes ($y=-5.5x+1{,}300$). **B** Relationship between hydrodynamic radii (R_H) and TEM-derived particle sizes ($y=1.37x-29$). The *gray line* corresponds to the identity line ($y=1.00x+0$)

most of the lipoprotein samples lie within their theoretical range, but all of the LDL_2 fractions had a hydrodynamic radius slightly smaller than the minimum expected value.

Although we found a high degree of correlation between the two techniques, their agreement was moderate in terms of absolute values (RMSPE of 20%). This is not surprising: The relationship between measured diffusion coefficient and particle size is complicated by obstruction effects, polydispersity, shape and flexibility effects, and other limitations of the simple Stokes–Einstein model. Of these problems, polydispersity is expected to be one of the most serious. The signal measured in an NMR experiment like DOSY is proportional to the number of spins present, so larger particles will contribute much more strongly to the NMR data than smaller, in proportion to the cube of the radius [36]. Thus, the diffusion coefficient obtained by NMR is expected to correspond to an "average" size larger than the mean of the radii obtained by TEM.

To assess the importance of polydispersity, we simulated an attenuating NMR dataset, corresponding to the parameters used for the experimental measurements, for each sample, using the experimental size distributions found with TEM (see Electronic Supplementary Material Appendix). These datasets were then fitted to the Stokes–Einstein equation as above and used to derive apparent hydrodynamic radii. For each sample, a correction factor for the effects of polydispersity on the NMR data was then calculated from the ratio of the mean TEM size listed in Table 1 to the size obtained by fitting the synthetic data. Finally, this correction factor was applied to the NMR data, allowing the TEM size to be compared to the NMR sizes corrected for the bias introduced by polydispersity. Figure 5 shows the linear regression between the corrected hydrodynamic radii obtained from NMR and the mean TEM sizes. As can be seen, this correction not only improved the correlation between the two techniques ($r^2=0.96$) but also improved the agreement (RMSPE of 15%), suggesting that the dominant systematic factor leading to differences in apparent size was polydispersity. It must be stressed that this correction was aimed at evaluating the importance of polydispersity in the agreement between the two techniques, and that it is not expected to be used routinely. It should perhaps be noted that there is no reason a priori to prefer the bias towards small particles inherent in using average TEM radius to the bias towards larger particles inherent in DOSY, if a single size parameter rather than a distribution is to be used: it does however mean that comparisons between the two require care.

Discussion

A previous study by O'Neal et al. used light scattering (LS) methods to determine the hydrodynamic radii of LDL lipoproteins [37]. LS methodology also determines the diffusion coefficients of lipoprotein fractions and uses the Stokes–Einstein equation to derive their hydrodynamic radii. However, in this study, a constant viscosity was considered. Sakurai et al. used the same technique to obtain the hydrodynamic radii of two LDL subclasses that were collected by ultracentrifugation [38]. Mean particle sizes of 108 and 102 Å for LDL_1 and LDL_2, respectively, were obtained. In our study, the mean particle sizes for the LDL_1 and LDL_2

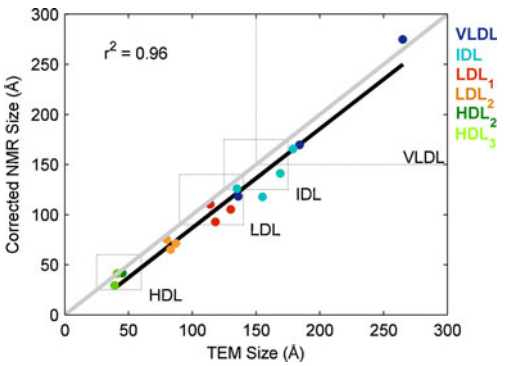

Fig. 5 Regression between corrected NMR sizes and mean TEM sizes ($y=0.99x-12$). The *gray line* corresponds to the identity line ($y=1.00x+0$)

subclasses were 114 and 87 Å, respectively. Thus, our approach seems to obtain relatively lower particle sizes for the LDL_2 fraction.

Although the experimental viscosity measured for this study, under stress conditions, does not necessarily correspond to the effective viscosity experienced by diffusing particle, the improvement in the correlation between NMR and TEM radii when the experimental viscosity is used in Eq. 3 suggests that this does provide an effective correction for the presence of solutes, including the lipoprotein. A more important reason for systematic differences between radii estimated by TEM and by NMR, however, is the polydispersity evidenced in the TEM data (see Electronic Supplementary Material Fig. S1–S7). The methyl signal fitted to obtain the diffusion coefficient is a composite containing contributions from all the different lipoprotein sizes present in the sample. The diffusion coefficients obtained by NMR are thus the result of an averaging over all the lipoprotein present [36]. Here, we have demonstrated that the diffusion coefficients obtained by NMR accurately reflect the distribution of sizes seen in TEM data, the NMR results showing a greater contribution from slower (larger) particles. The method described here thus yields more reliable values than previous studies, in which a constant value for the viscosity was used and no corrections for polydispersity were attempted.

Conclusions

In this study, DOSY experiments were carried out on lipoprotein fractions to assess their average particle sizes. The diffusion coefficients thus obtained had low estimation errors, demonstrating the repeatability of this technique. The hydrodynamic radii found when using the experimental viscosity in the Stokes–Einstein equation were highly correlated with the mean TEM sizes, although there was a systematic difference between the TEM and NMR-derived sizes. This systematic difference was shown to be explained by the polydisperse distributions found by TEM; once this was taken into account, a high degree of agreement was obtained between the two techniques. We propose that NMR is a potentially useful alternative to other available approaches for measuring lipoprotein fraction particle sizes, due to its inherent robustness and minimal sample manipulation.

Acknowledgments We acknowledge CIBER de Diabetes y Enfermedades Metabólicas Asociadas (ISCIII, Ministerio de Ciencia e Innovación), for partially funding this work, as well as the FIS (project PI 081409). This work was partly supported by the Engineering and Physical Sciences Research Council (Grant Numbers EP/H024336/1 and EP/I007989/1). We also acknowledge Dr. M. Moncusí and Dr. R. Marimon for their assistance with the TEM analysis of the lipoprotein fractions as well as Dr. S. Pujol for her assistance with viscosity measurements.

References

1. Krauss RM (2010) Lipoprotein subfractions and cardiovascular disease risk. Curr Opin Lipidol 21:305–311
2. Berneis KK, Krauss RM (2002) Metabolic origins and clinical significance of LDL heterogeneity. J Lipid Res 43:1363–1379
3. Musunuru K, Orho-Melander M, Caulfield MP, Li SG, Salameh WA, Reitz RE, Berglund G, Hedblad B, Engstrom G, Williams PT, Kathiresan S, Melander O, Krauss RM (2009) Ion mobility analysis of lipoprotein subfractions identifies three independent axes of cardiovascular risk. Arterioscler Thromb Vasc Biol 29:1975–U1628
4. Campos H, Genest JJ, Blijlevens E, McNamara JR, Jenner JL, Ordovas JM, Wilson PWF, Schaefer EJ (1992) Low-density-lipoprotein particle-size and coronary-artery disease. Arterioscler Thromb 12:187–195
5. Coresh J, Kwiterovich PO, Smith HH, Bachorik PS (1993) Association of plasma triglyceride concentration and LDL particle diameter, density, and chemical-composition with premature coronary-artery disease in men and women. J Lipid Res 34:1687–1697
6. Roheim PS, Asztalos BF (1995) Clinical-significance of lipoprotein size and risk for coronary atherosclerosis. Clin Chem 41:147–152
7. Krauss RM (1995) Dense low-density lipoproteins and coronary-artery disease. Am J Cardiol 75:B53–B57
8. Glomset JA (1968) Plasma lecithin—cholesterol acyltransferase reaction. J Lipid Res 9:155–167
9. Johnson WJ, Mahlberg FH, Rothblat GH, Phillips MC (1991) Cholesterol transport between cells and high-density-lipoproteins. Biochim Biophys Acta 1085:273–298
10. Stampfer MJ, Sacks FM, Salvini S, Willett WC, Hennekens CH (1991) A prospective-study of cholesterol, apolipoproteins, and the risk of myocardial-infarction. N Engl J Med 325:373–381
11. Stampfer MJ, Krauss RM, Ma J, Blanche PJ, Holl LG, Sacks FM, Hennekens CH (1996) A prospective study of triglyceride level, low-density lipoprotein particle diameter, and risk of myocardial infarction. Jama-J Am Med Assoc 276:882–888
12. Sacks FM, Campos H (2003) Clinical review 163—cardiovascular endocrinology 4—low-density lipoprotein size and cardiovascular disease: a reappraisal. J Clin Endocrinol Metab 88:4525–4532
13. Mora S, Otvos JD, Rifai N, Rosenson RS, Buring JE, Ridker PM (2009) Lipoprotein particle profiles by nuclear magnetic resonance compared with standard lipids and apolipoproteins in predicting incident cardiovascular disease in women. Circulation 119:931–U944
14. Kulkarni KR, Garber DW, Marcovina SM, Segrest JP (1994) Quantification of cholesterol in all lipoprotein classes by the VAP-II method. J Lipid Res 35:159–168
15. Jeyarajah EJ, Cromwell WC, Otvos JD (2006) Lipoprotein particle analysis by nuclear magnetic resonance spectroscopy. Clin Lab Med 26:847–870
16. Krauss RM, Burke DJ (1982) Identification of multiple subclasses of plasma low-density lipoproteins in normal humans. J Lipid Res 23:97–104
17. Hoefner DM, Hodel SD, O'Brien JF, Branum EL, Sun D, Meissner I, McConnell JP (2001) Development of a rapid, quantitative method for LDL subfractionation with use of the Quantimetrix Lipoprint LDL System. Clin Chem 47:266–274
18. Witte DR, Taskinen MR, Perttunen-Nio H, van Tol A, Livingstone S, Colhoun HM (2004) Study of agreement between LDL size as measured by nuclear magnetic resonance and gradient gel electrophoresis. J Lipid Res 45:1069–1076
19. Ensign W, Hill N, Heward CB (2006) Disparate LDL phenotypic classification among 4 different methods assessing LDL particle characteristics. Clin Chem 52:1722–1727

20. McNamara JR, Warnick GR, Cooper GR (2006) A brief history of lipid and lipoprotein measurements and their contribution to clinical chemistry. Clin Chim Acta 369:158–167
21. Chung M, Lichtenstein AH, Ip S, Lau J, Balk EM (2009) Comparability of methods for LDL subfraction determination: a systematic review. Atherosclerosis 205:342–348
22. Mora S (2009) Advanced lipoprotein testing and subfractionation are not (yet) ready for routine clinical use. Circulation 119:2396–2404
23. Rosenson RS, Brewer HB, Chapman MJ, Fazio S, Hussain MM, Kontush A, Krauss RM, Otvos JD, Remaley AT, Schaefer EJ (2011) HDL measures, particle heterogeneity, proposed nomenclature, and relation to atherosclerotic cardiovascular events. Clin Chem 57:392–410
24. Johnson CS (1999) Diffusion ordered nuclear magnetic resonance spectroscopy: principles and applications. Prog Nucl Magn Reson Spectrosc 34:203–256
25. Antalek B (2002) Using pulsed gradient spin echo NMR for chemical mixture analysis: how to obtain optimum results. Concepts Magn Reson 14:225–258
26. Morris GA (2007) Diffusion-ordered spectroscopy (DOSY). Wiley, New York
27. Hinton DP, Johnson CS (1993) Diffusion ordered 2D-NMR spectroscopy of phospholipid-vesicles—determination of vesicle size distributions. J Phys Chem 97:9064–9072
28. Canzi G, Mrse AA, Kubiak CP (2011) Diffusion-ordered NMR spectroscopy as a reliable alternative to TEM for determining the size of gold nanoparticles in organic solutions. J Phys Chem C 115:7972–7978
29. Squires TM, Mason TG (2010) Fluid mechanics of microrheology. Annu Rev Fluid Mech 42:413–438
30. Forte TM, Nordhausen RW (1986) Electron-microscopy of negatively stained lipoproteins. Methods Enzymol 128:442–457
31. Schumaker VN, Puppione DL (1986) Sequential flotation ultracentrifugation. Methods Enzymol 128:155–170
32. Rumsey SC, Galeano NF, Arad Y, Deckelbaum RJ (1992) Cryopreservation with sucrose maintains normal physical and biological properties of human plasma low-density lipoproteins. J Lipid Res 33:1551–1561
33. Jerschow A, Muller N (1997) Suppression of convection artifacts in stimulated-echo diffusion experiments. Double-stimulated-echo experiments. J Magn Reson 125:372–375
34. Mallol R, Rodríguez M, Heras M, Vinaixa M, Cañellas N, Brezmes J, Plana N, Masana L, Correig X (2011) Surface fitting of 2D diffusion-edited 1H NMR spectroscopy data for the characterisation of human plasma lipoproteins. Metabolomics 7:572–582
35. Duell PB, Illingworth DR, Connor WE (2001) Endocrinology and metabolism, 4th edn. McGraw-Hill, New York
36. Chen A, Wu DH, Johnson CS (1995) Determination of molecular-weight distributions for polymers by diffusion-ordered NMR. J Am Chem Soc 117:7965–7970
37. O'Neal D, Harrip P, Dragicevic G, Rae D, Best JD (1998) A comparison of LDL size determination using gradient gel electrophoresis and light-scattering methods. J Lipid Res 39:2086–2090
38. Sakurai T, Trirongjitmoah S, Nishibata Y, Namita T, Tsuji M, Hui SP, Jin S, Shimizu K, Chiba H (2010) Measurement of lipoprotein particle sizes using dynamic light scattering. Ann Clin Biochem 47:476–481